Available online at www.sciencedirect.com
ScienceDirect
Ceramics International 37 (2011) 2061–2068
CERAMICS INTERNATIONAL
www.elsevier.com/locate/ceramint

Review paper

Sb doping effects on the piezoelectric and ferroelectric characteristics of lead-free $Na_{0.5}K_{0.5}Nb_{1-x}$ Sb_xO_3 piezoelectric ceramics

I-Hao Chan [a], Chieh-Tze Sun [b], Mau-Phon Houng [a,*], Sheng-Yuan Chu [b,c,**]

[a] Institute of Microelectronics, Department of Electrical Engineering, National Cheng Kung University, Tainan 701, Taiwan
[b] Department of Electrical Engineering, National Cheng Kung University, Tainan 701, Taiwan
[c] Center for Micro/Nano Science and Technology, National Cheng Kung University, Tainan 701, Taiwan

Received 12 February 2011; received in revised form 25 April 2011; accepted 28 April 2011
Available online 6 May 2011

Abstract

The piezoelectric, phase structure and ferroelectric properties of lead-free $Na_{0.5}K_{0.5}Nb_{1-x}Sb_xO_3$ piezoelectric ceramics were systematically investigated. $(Na_{0.5}K_{0.5})Nb_{1-x}Sb_xO_3$ ceramics were synthesized using the conventional solid-state reaction method. The effect of B-site Sb^{5+} substitution for Nb^{5+} on the structural characteristics and piezoelectric properties of samples was determined. According to XRD patterns, the phase gradually changes from tetragonal to orthorhombic with increasing Sb content. At $x = 0.03$, the tetragonal and orthorhombic phases coexist and relatively high piezoelectric properties were obtained. The relatively high Q_m value obtained after substitution with Sb^{5+} ions might be due to the increased electronegativity and decreased ionic radius at the morphotropic phase boundary (MPB) at $x = 0.03$. However, the Q_m value decreases with further Sb addition. Relatively high piezoelectric properties at $x = 0.03$ of $k_p = 0.42$, $k_t = 0.48$, $\varepsilon_r = 446$, $Q_m = 143$, $\tan\delta = 2.3\%$, and density = 4.31 g/cm^3, $d_{33} = 123$ pC/N, were obtained.

Keywords: NKN; Lead-free; Piezoelectric

Contents

1. Introduction

Lead-based $Pb(ZrTi)O_3$ piezoelectric ceramics are widely used in piezoelectric devices such as actuators and sensors [1,2], surface acoustic wave filters (SAW) [3], transducers [4], buzzers [5], and piezoelectric transformers [6,7] due to their

* Corresponding author. Tel.: +886 6 2757575x62342; fax: +886 6 2094786.
** Corresponding author at: Department of Electrical Engineering, National Cheng Kung University, Tainan 701, Taiwan. Tel.: +886 6 2757575x62381; fax: +886 6 2345482.
E-mail address: chusy@mail.ncku.edu.tw (S.-Y. Chu).

0272-8842/$36.00
doi:10.1016/j.ceramint.2011.04.120

excellent electrical properties and temperature stability. However, lead-based piezoelectric ceramics cause environmental pollution and health problems because of the high toxicity of PbO evaporation. A lot of countries have recently limited the use of lead-based products. A replacement for lead-based piezoelectric ceramics is thus required.

Many lead-free piezoelectric ceramic systems have been studied, such as Bi compounds [8,9], (Na,K)NbO_3 [10,11], and $BaTiO_3$ [12,13]. Among lead-free piezoelectric ceramics, (Na,K)NbO_3-based ceramic systems have attracted a lot of attention as replacements for lead-based ceramics due to their excellent piezoelectric properties, high Curie temperature, and relatively low harm to the environment. It is well known that pure NKN ceramics are difficult to synthesize using the conventional solid state reaction method through an ordinary sintering process and that they easily decompose when exposed to air and moisture due to the evaporation of alkaline elements under high sintering temperature. When the sintering temperature is above 1000 °C, the evaporation of K_2O and Na_2O degrades the resistivity and the piezoelectric properties. However, it is very difficult to control the evaporation of Na_2O and K_2O by muffling. Therefore, new methods are needed to maintain the electrical and piezoelectric properties of NKN-based samples, such as adjusting the K/Na ratio or A/B site ratio for the optimal proportion [14–17] or lowering the sintering temperature to under 1000 °C by doping the samples with extrinsic materials [18].

Several researches have been made by doping extrinsic material to increase the piezoelectric properties (k_p, k_t, density, Q_m, loss) or decrease the aging effect. Dopants such as $LiTaO_3$ [18,19], CuO [18,20], ZnO [20], $LiSbO_3$ [21], $LiNbO_3$ [22], $BaTiO_3$ [23], $SrTiO_3$ [24], $CaTiO_3$ [25], $AgTaO_3$ [26], Fe_2O_3 [27], and Sb_2O_5 [28] have been added to NKN-based ceramics to form new NKN-based ceramic systems. The (Na,K)(Nb,Sb) system is a candidate for replacing pure NKN lead-based ceramics. Lin et al. reported that for the (Na,K)(Nb,Sb)–MnO_2 [29] system, a small amount of MnO_2 is enough to improve the densification, ferroelectric, and piezoelectric properties. Dambekalne et al., studied the (Na,K)(Nb,Sb)–MnO_2 [30] system, and found that MnO_2 functions as a sintering aid and effectively improves densification. Wu et al. researched the (Na,K)(Nb,Sb)–$CaTiO_3$ [31] system; their results show that $CaTiO_3$-modified (Na,K)(Nb,Sb) lead-free piezoelectric ceramics form a stable solution with an orthorhombic structure and that the piezoelectric properties of the ceramics strongly depend on the poling temperature. Park et al. investigated the (Na,K)(Nb,Sb)–CuO [32] system. A small number of Cu^{2+} ions were incorporated into the matrix of the NKNS ceramics and behaved as a hardener. Su et al. studied the (Na,K)(Nb,Sb) [33] system that the (Na,K)(Nb,Sb) lead-free peizoelectric ceramic powders were successfully synthesized by hydrothermal treatment with substituting Sb for Nb.

However, there are few studies have investigated the effect of Sb doping in NKNS ceramics. In this presented study, the effect of Sb^{5+} added to NKN-based ceramics to substitute Nb^{5+} on the structure and electrical characteristics is investigated. The improvement of piezoelectric and ferroelectric properties of samples is also discussed.

2. Experiment

2.1. Sample preparation

The raw materials used to prepare the samples of $K_{0.5}Na_{0.5}Nb_{1-x}Sb_xO_3$, $x = 0$–0.1 using a conventional mixed-oxide method were pure reagent Na_2CO_3 (SHOWA, 99.5%), K_2CO_3 (SHOWA, 99.5%), Nb_2O_5 (SHOWA, 99.5%), and Sb_2O_5 (Alfa Aesar, 99.998%) powders. Na_2CO_3 and K_2CO_3 were first placed in a stove at 130 °C to remove water. Then, $K_{0.5}Na_{0.5}Nb_{1-x}Sb_xO_3$ (NKNS) was weighed according to the desired composition. The starting materials were individually transferred to a 100-mm-diameter cylindrical plastic jar partially filled with 10-mm-diameter ZrO_2 grinding balls. Sufficient ethanol (99.5%) was added to cover the powders. Ball milling was carried out for 24 h, followed by drying at 130 °C and grinding using an alumina mortar and pestle to break up large agglomerates formed during drying. The stoichiometric NKNS powders were first synthesized at 850 °C for 5 h using a solid-state reaction method. After calcination,

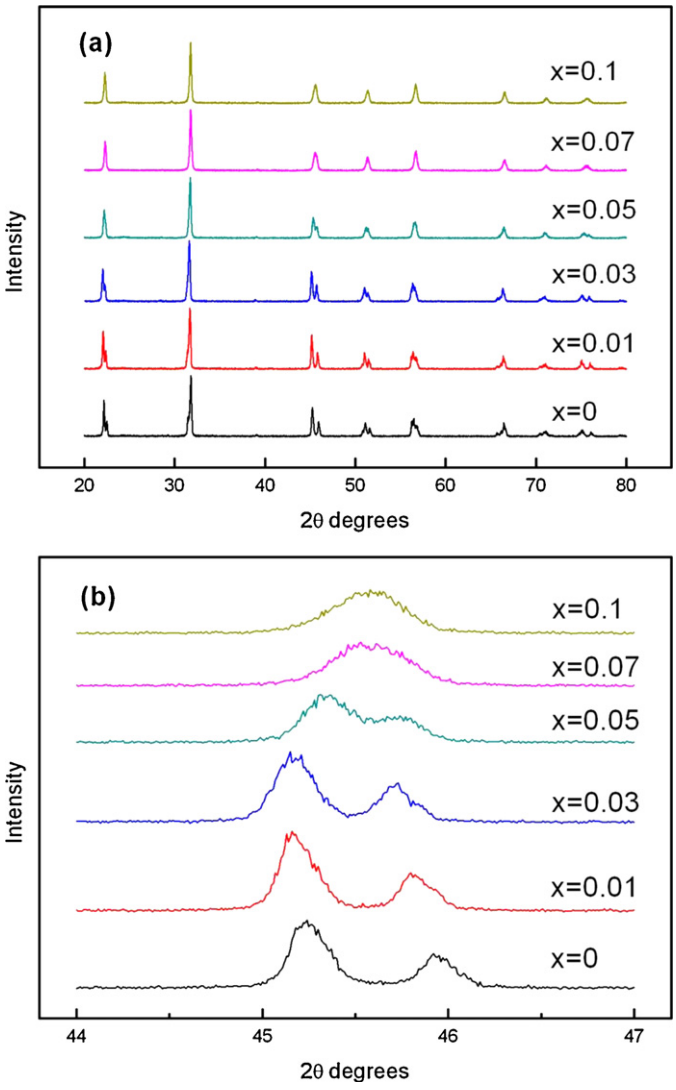

Fig. 1. X-ray of $(Na_{0.5}K_{0.5})(Nb_{1-x}Sb_x)$ lead-free ceramics for $x = 0$–0.1. (a) $\theta = 20$–80° and (b) $\theta = 44$–47°.

NKNS powders were weighed according to the formula of NKNS and ball milled for 24 h again. After being dried, the powders were milled with 5 wt% PVA aqueous solution, and then uni-axially pressed into 12-mm-diameter disks at a pressure of 25 kg/cm^2. After de-binder the disks were sintered in air at 1000–1100 °C for 2 h. Bulk densities were measured using the Archimedes method with D.I. water as a medium.

2.2. Sample characterization

The microstructure was observed using field emission scanning electron microscopy (FESEM, Hitachi S-4100). The crystallographic study was confirmed by X-ray diffraction (XRD) using CuK_α (λ = 0.154 nm) radiation with a Seimens D-5000 diffractometer operated at 40 kV and 40 mA. The dielectric and piezoelectric properties were measured with an HP 4294A precision impedance analyzer. To measure the electrical properties, silver paste was painted on both sides of the samples as electrodes. The samples were subsequently fired at 130 °C for 20 min. After firing, samples were poled under a 30 kV/cm DC field at 120 °C in a silicone oil bath for 30 min. The electromechanical coupling factors of thickness (k_t) and planar (k_p) modes were calculated using the resonance and anti-resonance method [18]. The coercive electric field (E_c) and the remnant polarization (P_r) were obtained under a 50 kV/cm AC field at 60 Hz using a modified Sawyer-Tower circuit. In order to prevent arcing, the samples were submerged in 120 °C silicon oil.

3. Results and discussion

3.1. XRD patterns and analysis

The XRD patterns of $N_{0.5}K_{0.5}N_{1-x}S_x$ ceramics with various x values sintered at 1000–1100 °C are shown in Fig. 1(a). All specimens had a perovskite structure without a second phase, indicating that the Nb^{5+} ions were successfully substituted by Sb^{5+} ions. In the 2-theta range of 45–47° (see Fig. 1(b)), the two diffraction peaks (0 0 2 and 2 0 0) start to merge when x is about 0.03, almost becoming one peak at x = 0.1, which indicates that the structure of the crystal changed. It could be seen that the diffraction peaks is shifting to higher angles, while the amount Sb is increasing. This phenomenon indicates that the volume of the lattice has slight shrinkage due to the different ion radius of Sb and Nb ions (CN = 6, R_{Sb} = 0.61, R_{Nb} = 0.64). In the previous studies about NKN the structure of NKN is orthorhombic at room temperature. When $x > 0.7$ the structure of NKNS is apparently changing. The splits diffraction peaks (0 0 2) and (2 0 0) merge gradually with increasing x value. The XRD indicates that the NKN ceramics transformed from a tetragonal phase into a rhombohedral–tetragonal structure; the tetragonal phase completely transformed into the rhombohedral phase as the doping concentration of Sb^{5+} was gradually increased [34].

The same phenomenon was observed in the 2-theta range of 52–72°. It indicates that the phase transition takes place at x = 0.03. In Fig. 1, no second phase was found, which suggests that Sb had already incorporated into the NKN matrix to replace Nb and that it had a perovskite structure.

3.2. Piezoelectric properties of $KNN_{1-x}S_x$ samples (x = 0, 0.01, 0.03, 0.05, 0.07, 0.1)

The electromechanical planar coefficient (k_p) and thickness coupling coefficient (k_t) of the $NKN_{1-x}Sb_x$ ceramics are shown in Fig. 2. The k_p and k_t were calculated using the following equation (1) [18,35]:

$$\frac{1}{k^2} = a \times \frac{f_r}{f_a - f_r} + b \quad (1)$$

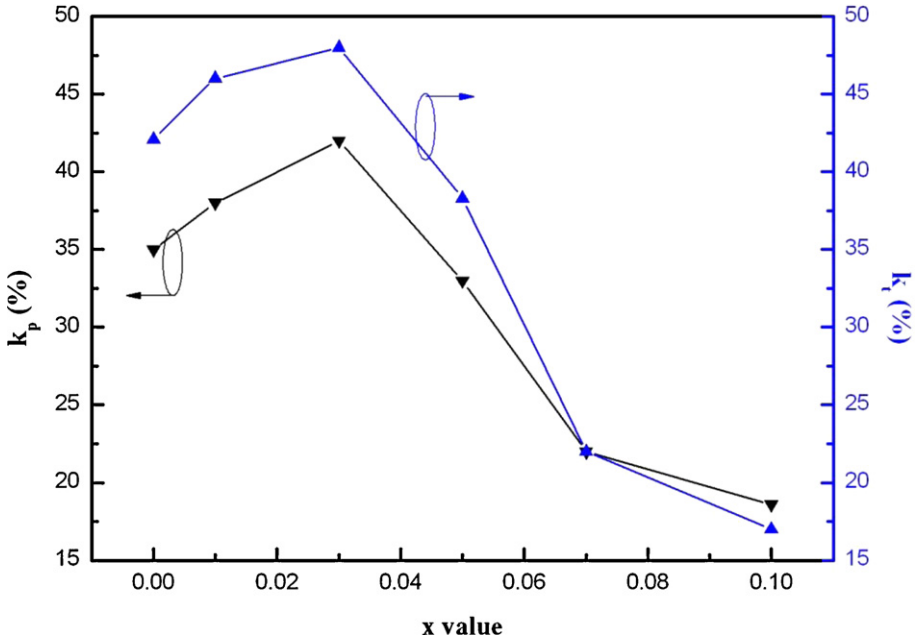

Fig. 2. k_p and k_t values for various values of x.

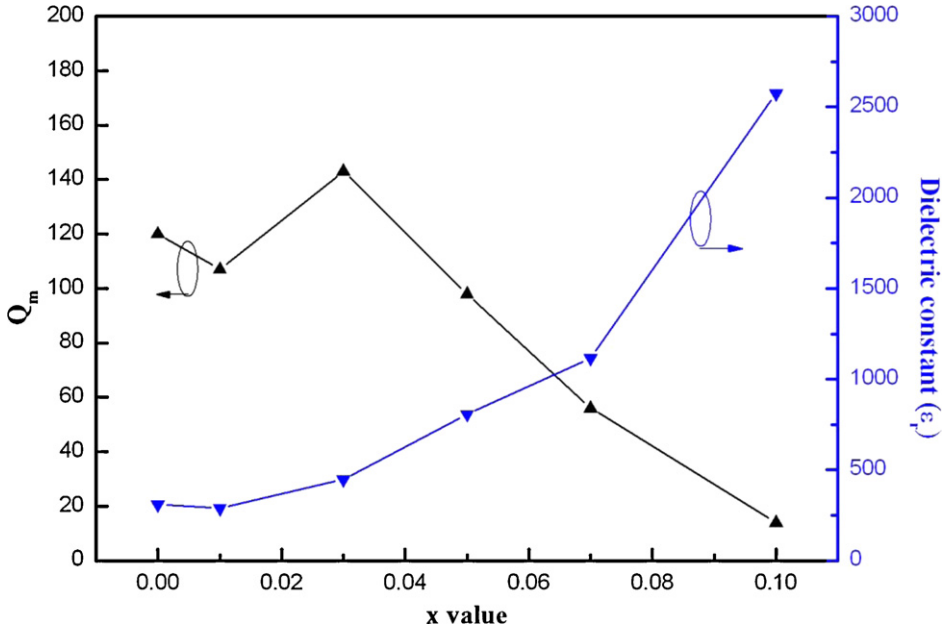

Fig. 3. Mechanical quality factor and dielectric constant for various values of x.

where f_r is the resonance frequency, f_a is the anti-resonance frequency, $a = 0.395$ and $b = 0.574$ for planar mode (k_p), and $a = 0.405$ and $b = 0.810$ for thickness mode (k_t). Longitudinal coupling, k_{33}, was estimated from the piezoelectric planar coefficient (k_p) and thickness coupling coefficient (k_t) [36]:

$$k_{33}^2 = k_p^2 + k_t^2 - k_p^2 k_t^2 \tag{2}$$

The values of Q_m shown in Fig. 3 were determined using the following equation (3) [35]:

$$\frac{1}{Q_m} = 2\pi f_r RC \frac{f_a^2 - f_r^2}{f_a^2} \tag{3}$$

where R is the resonance impedance and C is the capacitance at 1 kHz. The maximum value of k_p of the $NKN_{1-x}Sb_x$ ceramics is about 42.2% and that of k_t is ~48% when $x = 0.03$, k_p and k_t increase with increasing B-site substitution amount of Sb when $x < 0.03$, whereas they decrease rapidly with increasing B-site substitution amount of Sb when $x > 0.03$. Sb dopant in NKN-based ceramics enhances both k_p and k_t.

Fig. 3 shows the Sb doping effect on Q_m, dielectric constant, and piezoelectric coefficient of samples. When $x = 0.01$, the mechanical quality factor is about 107; it reaches a maximum value of 143 when $x = 0.03$, and then decreases with increasing amount of Sb.

The different electronegativity between Sb and Nb (Sb: 2.05, Nb: 1.6), can increase the electronegativity by selecting Sb to substitute for Nb. The Sb–O bond is known to be shorter and stronger than the Nb–O bond because the electronegativity of Sb element (2.05) is higher than that of Nb (1.6). Owning to the substitution the ferroelectricity can be increased with the raising x value then decreased when x exceeded 0.03 [32,33]. The smaller ionic size of Sb^{5+} ions ($R_{Sb} = 0.61$ Å, $R_{Nb} = 0.64$ Å) makes the B-site cations falling off from the center [29,37]. The increasing ferroelectricity and decreased B-site ionic radius increase the covalency and the B-site cations falling off from the center. Moreover, the enhanced ferroelectricity, covalency, and falling off of the center cations can improve the poling conditions of the $Na_{0.5}K_{0.5}Nb_{1-x}S_x$ ceramics.

The increased Q_m value with Sb^{5+} ion substitution might be explained by the increased electronegativity and decreased ionic radius. However, the Q_m value decreased with further Sb addition, as shown in Fig. 3, which is probably due to the decreased ferroelectricity caused by the specimens changing from the orthorhombic phase to the cubic phase with increasing Sb content when $x > 0.03$. Therefore, it was considered that the $N_{0.5}K_{0.5}N_{1-x}S_x$ ceramics had the appropriate poling state and achieved high Q_m result at $x = 0.03$. The detailed piezoelectric properties of the samples are shown in Table 1.

3.3. P–E hysteresis loops

Fig. 4 shows the relative density and tan δ values of $N_{0.5}K_{0.5}N_{1-x}S_x$ ceramics with $0 \le x \le 0.1$ sintered at 1075 °C for 2 h. The relative density of the NKNS ceramics sintered at 1075 °C was about 95% of the theoretical density, and increased slightly with increasing Sb content, indicating that all the specimens were well densified at this temperature. With increasing Sb content, tan δ values of specimens increased, which indicates that NKNS ceramics became soft piezoelectric ceramics.

The P–E hysteresis loops of $NKN_{1-x}Sb_x$ ceramics are shown in Fig. 5. All the specimens were measured at 120 °C and 60 Hz in a silicon oil sink. The observed P–E hysteresis loops data were recorded from the oscilloscope. When $x = 0.03$, the loop has a relatively square shape in which the higher P_r and field E_c occurred. The remnant polarization P_r and the coercive field E_c variations with x for the $NKN_{1-x}Sb_x$ ceramics are listed in Table 2.

Table 1
Piezoelectric properties of $NaKNb_{1-x}Sb_x$ lead-free ceramics with $0 \leq x \leq 0.1$.

x	0	0.01	0.03	0.05	0.07	0.1
k_p	0.35	0.38	0.42	0.33	0.22	0.18
k_t	0.42	0.46	0.48	0.38	0.22	0.17
Q_m	120	107	143	98	56	14
D (g/cm^3)	4.29	4.17	4.31	4.27	3.9	3.6
ε_r	309	288.4	446.5	806	1116	2575
loss	0.015	0.024	0.023	0.035	0.042	0.063
k_{33}	0.547	0.597	0.638	0.506	0.3111	0.252

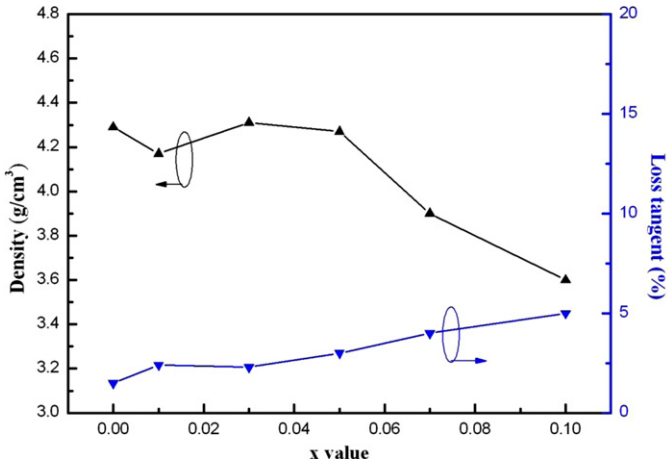

Fig. 4. Density and tan δ for various values of x.

It was found that P_r and E_c varying with x value. P_r increases in the beginning and then decreases with a maximum value at $x = 0.03$; relatively high E_c reaches 17.2 kV/cm and polarization $P_r = 11.03$ μC/cm^2 are obtained at $x = 0.03$ which confirms the coexistence of orthorhombic and tetragonal phases in $NKN_{1-x}Sb_x$ ceramics. The coexistence of orthorhombic and tetragonal phases plays an important role in improving the ferroelectric properties and poling state. Moreover, it was found that the trend of P_r with Sb content is similar to the variation of the bulk density of $NKN_{1-x}Sb_x$ ceramics. These results indicate

Table 2
P_r and E_c of the $NKN_{1-x}Sb_x$ ceramics lead-free ceramics with $0 \leq x \leq 0.07$.

x	0	0.01	0.03	0.07
P_r (μC/cm^2)	4.52	2.97	11.03	12.7
E_c (kV/cm)	9.3	9.5	17.2	11.3

that the increasing Q_m is due to the decrease of the leakage current and enhancing the polarization state, which leads the P–E loop become relatively square. It confirms that the structure of the NKNS piezoelectric ceramics is changing along with the increase x value.

3.4. Dielectric constant and Curie temperature

Fig. 6 shows the dielectric constant of $NKN_{1-x}Sb_x$ ceramics. The Curie temperature (T_C) and the transition temperature of the orthorhombic and tetragonal phases (T_{O-T}) both decreased with increasing x values. The decrease of T_C was faster than that of T_{O-T}. Hence, the tetragonal region shrinks with increasing Sb^{5+} content, as shown in Fig. 7. When the x value achieved 0.1 eventually, the specimen changes gradually from a ferroelectric structure to a relaxor-type structure [32,34]. According to Fig. 6, the measured dielectric constant peak value at the Curie temperature decreased with increasing Sb content and T_C shifted to a lower temperature. In contrast, the dielectric

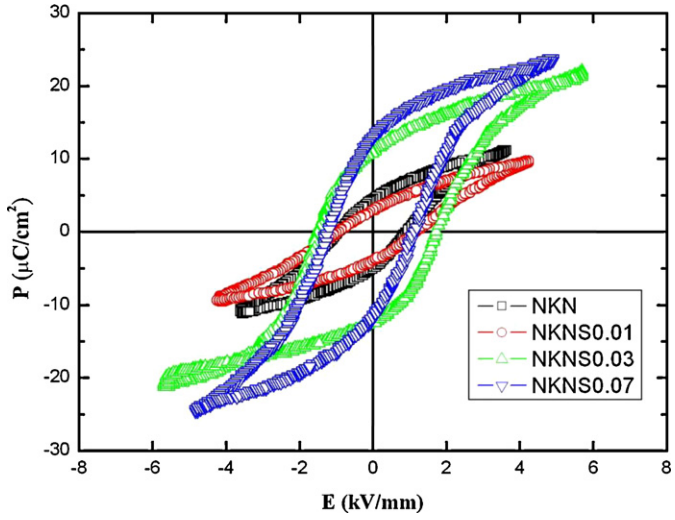

Fig. 5. P–E loop of NKNS ceramics for various values of x.

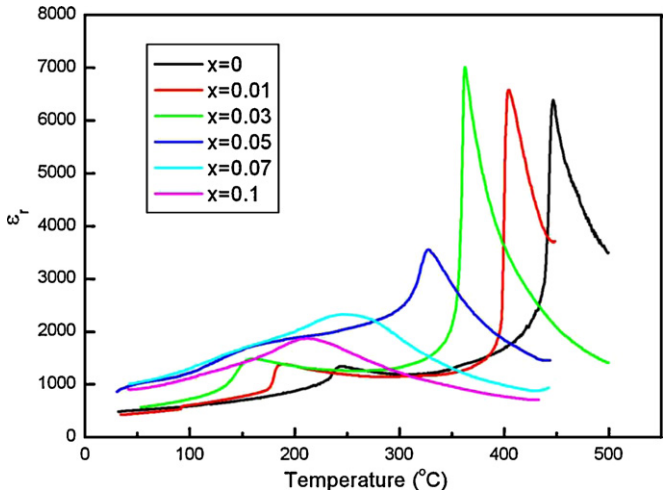

Fig. 6. Dielectric constant versus temperature of $N_{0.5}K_{0.5}N_{1-x}S_x$ for various values of x.

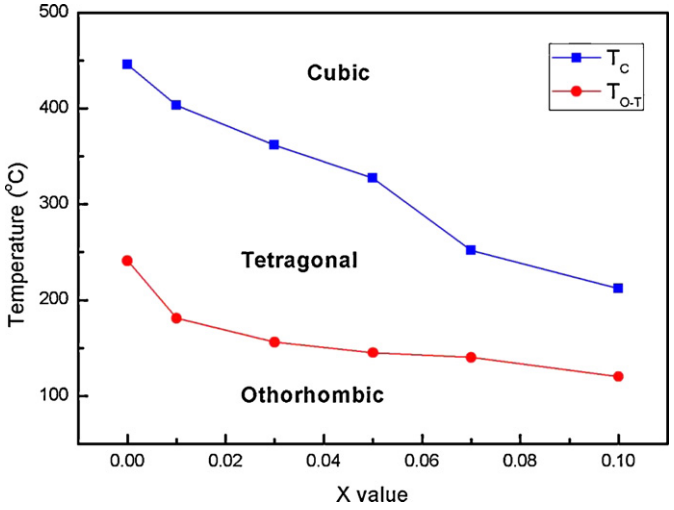

Fig. 7. T_C point and $T_{O–T}$ point of $N_{0.5}K_{0.5}N_{1-x}S_x$ for various values of x.

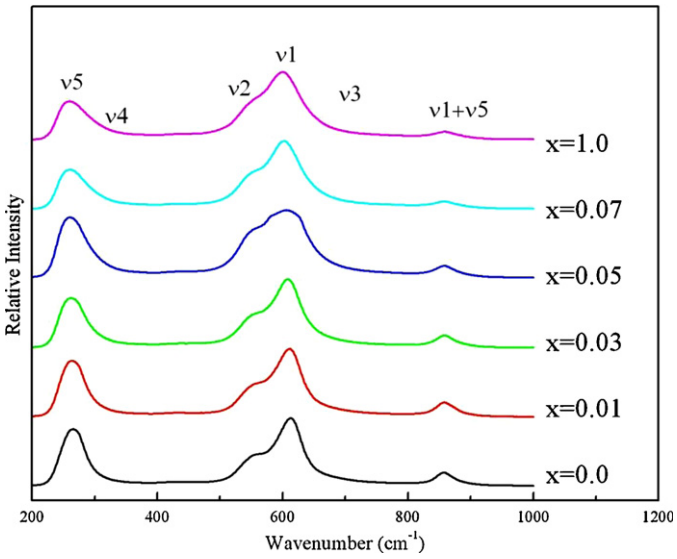

Fig. 8. Raman spectra of $N_{0.5}K_{0.5}N_{1-x}S_x$ ceramics measured at room temperature.

constant peak value measured at $T_{O–T}$ increased with increasing Sb content and $T_{O–T}$ shifted slightly to a lower temperature. The shift in T_C is significantly faster than that in $T_{O–T}$. When $x < 0.03$, T_C is very distinct. For $x > 0.03$, it becomes smooth and obscure, like that of a relaxor. The same trend was found for $T_{O–T}$, but unlike T_C, it moves to a lower temperature slowly. When x is higher than 0.03, the dielectric constant increases rapidly at room temperature. The transition temperature of T_C and $T_{O–T}$ slightly decreases with increasing x value. The decrease of the Curie temperature indicates that the Sb substitution makes the NKN-based ceramics transform into a relaxor-like structure and become soft piezoelectric ceramics.

3.5. Raman spectrum

XRD can confirm the macroscopic symmetry in long-range ordering and Raman spectroscopy is sensitive to non-uniform distortions of the crystal lattice in short-range ordering [25,33,38]. In this work, the Sb-doping in the B sites may greatly distort the perovskite structure due to the Sb–O bond shorter and stronger than that of Nb–O because the electronegativity of Sb (2.05) is higher than Nb (1.6). Ahtee and Glazer [39,40] proposed that the octahedral tilting in the perovskite structures was mainly induced by a difference in the ionic radii between the A site and B site. The different ionic radius also caused the octahedral tilting. The distortive perovskite structure is formed with corner-sharing BO_6 octahedron and AO_{12} dodecahedron. Hence, the K and Na atoms may equally occupy the A site and be surrounded by 12 oxygen atoms with Sb and Nb atoms occupy the B site in the middle of the cell to form the $NKN_{1-x}Sb_x$ solid solution [33]. The Raman spectrum experiments measured at room temperature for the samples of $NKN_{1-x}Sb_x$ ceramics is shown in Fig. 8. According to the literature, the vibrations of a NbO_6 octahedron are made up of 1A1g(ν1) + 1Eg(ν2) + 2F1u(ν3,ν4) + F2g(ν5) + F2u(ν6) in this case, where ν means the frequency band and A1g, Eg, F1u, F1u, F2g, and F2u indicate six species of vibration modes) Among these vibrations, 1A1g(ν1) + 1Eg(ν2) + 1F1u(ν3) are stretching and the rest are bending modes. The figure shows the Raman spectra of $NKN_{1-x}Sb_x$ ceramics measured at room temperature. ν5 (262 cm^{-1}) and ν1 (616 cm^{-1}) are detected as relatively strong scattering. With increasing Sb content, the peaks for ν1 shift to a lower frequency and the full-width at half-maximum (FWHM) also becomes broader. This is due to the incorporation of Sb into the B-site, which increases the binding strength of O–Nb–O.

In Fig. 9 we can observe the d_{33} value of NKNS ceramics varies with the increasing Sb amount. The d_{33} value first increases then decreases with $x = 0$–0.1. A maximum $d_{33} = 123$ pC/N is measured when $x = 0.03$ which is in good agreement with the piezoelectric properties. When x is lower than 0.03, the d_{33} value of NKNS ceramics is increasing gradually. The d_{33} shows significant decreasing while $x > 0.05$ which is also in agreement with the low piezoelectric properties.

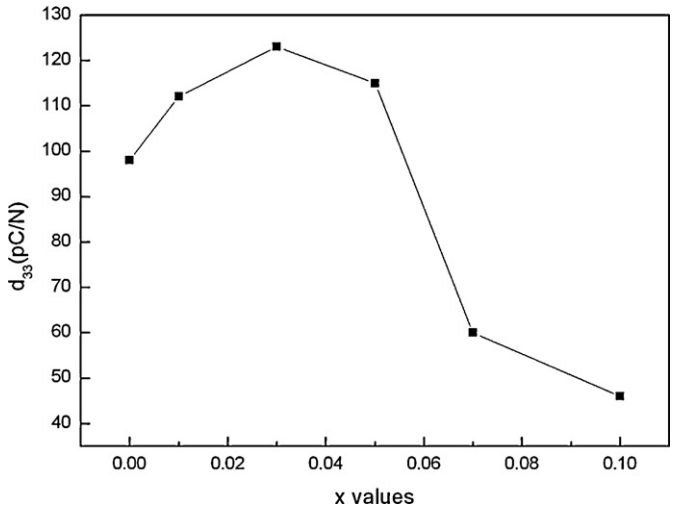

Fig. 9. The measurement d_{33} values of $N_{0.5}K_{0.5}N_{1-x}S_x$ for various x values.

4. Conclusion

In this study, the piezoelectric, phase structure, and ferroelectric properties of lead-free $Na_{0.5}K_{0.5}Nb_{1-x}Sb_xO_3$ piezoelectric ceramics fabricated using a conventional solid-state reaction method were investigated. The effect of B-site substitution of Sb^{5+} for Nb^{5+} was observed from XRD patterns. The phase structure of the ceramics gradually changed from tetragonal to orthorhombic with increasing x value. Relatively high piezoelectric properties were obtained when the tetragonal and orthorhombic phases coexisted (at $x = 0.03$). The relatively high Q_m value with Sb^{5+} ion substitution might be explained by the increased electronegativity and decreased ionic radius at the MPB at $x = 0.03$. However, the Q_m value decreased with further Sb addition and behaved like that of a relaxor. The following properties of $(Na_{0.5}K_{0.5})Nb_{0.97}$ $Sb_{0.03}O_3$ were obtained: $k_p = 0.42$, $k_t = 0.48$, $\varepsilon_r = 446$, $Q_m = 143$, $\tan\delta = 2.3$, density = 4.31, $d_{33} = 123$ pC/N.

Acknowledgement

The authors acknowledge the National Science Council (NSC) of the Republic of China (Taiwan) for financially supporting this research under Contract No. NSC-99-2221-E-017-005.

References

[1] T.-Y. Chen, S.-Y. Chu, C.-K. Cheng, Doping effects on the piezoelectric properties of low-temperature sintered $PbTiO_3$-based ceramics for SAW applications, Integrated Ferroelectrics 58 (2003) 1315–1324.
[2] S.-Y. Chu, T.-Y. Chen, W. Water, The investigation of preferred orientation growth of ZnO films on the $PbTiO_3$-based ceramics and its application for SAW devices, Journal of Crystal Growth 257 (2003) 280–285.
[3] S.-Y. Chu, T.-Y. Chen, I.T. Tsai, Effects of poling field on the piezoelectric and dielectric properties of Nb additive PZT-based ceramics and their applications on SAW devices, Materials Letters 58 (2004) 752–756.
[4] B. Jadidian, N. Hagh, A. Winder, A. Safari, 25 MHz ultrasonic transducers with lead-free piezoceramic, 1-3 PZT fiber-epoxy composite, and PVDF polymer active elements, IEEE Transactions on Ultrasonics Ferroelectrics and Frequency Control 56 (2009) 368–378.
[5] K.-T. Chang, H.-C. Chiang, C.-W. Lee, Design and implementation of a piezoelectric clutch mechanism using piezoelectric buzzers, Sensors and Actuators A: Physical 141 (2008) 515–522.
[6] Z. Yang, X. Chao, R. Zhang, Y. Chang, Y. Chen, Fabrication and electrical characteristics of piezoelectric PMN-PZN-PZT ceramic transformers, Materials Science and Engineering B: Solid-State Materials for Advanced Technology 138 (2007) 277–283.
[7] C.-W. Ahn, H.-C. Song, S. Nahm, S. Priya, S.-H. Park, K. Uchino, H.-G. Lee, H.-J. Lee, Effect of ZnO and CuO on the sintering temperature and piezoelectric properties of a hard piezoelectric ceramic, Journal of the American Ceramic Society 89 (2006) 921–925.
[8] T. Takenaka, T. Gotoh, S. Mutoh, T. Sasaki, New series of bismuth layer-structured ferroelectrics, Japanese Journal of Applied Physics Part 1: Regular Papers Short Notes and Review Papers 34 (1995) 5384–5388.
[9] M. Hirose, T. Suzuki, H. Oka, K. Itakura, Y. Miyauchi, T. Tsukada, Piezoelectric properties of $SrBi_4Ti_4O_{15}$-based ceramics, Japanese Journal of Applied Physics Part 1: Regular Papers Short Notes and Review Papers 38 (1999) 5561–5563.
[10] Y. Saito, H. Takao, T. Tani, T. Nonoyama, K. Takatori, T. Homma, T. Nagaya, M. Nakamura, Lead-free piezoceramics, Nature 432 (2004) 84–87.
[11] J. Acker, H. Kungl, M.J. Hoffmann, Influence of alkaline and niobium excess on sintering and microstructure of sodium–potassium niobate ($K_{0.5}Na_{0.5})NbO_3$, Journal of the American Ceramic Society 93 (2010) 1270–1281.
[12] O.P. Thakur, C. Prakash, A.R. James, Enhanced dielectric properties in modified barium titanate ceramics through improved processing, Journal of Alloys and Compounds 470 (2009) 548–551.
[13] C.-W. Ahn, D. Maurya, C.-S. Park, S. Nahm, S. Priya, A generalized rule for large piezoelectric response in perovskite oxide ceramics and its application for design of lead-free compositions, Journal of Applied Physics 105 (2009).
[14] S.-Y. Chu, W. Water, Y.-D. Juang, J.-T. Liaw, Properties of (Na, K)NbO_3 and (Li, Na, K)NbO_3 ceramic mixed systems, Ferroelectrics 287 (2003) 23–33.
[15] Q. Zhang, B. Zhang, H. Li, P. Shang, Effects of Na/K ratio on the phase structure and electrical properties of $Na_xK_{1-x}NbO_3$ lead-free piezoelectric ceramics, Rare Metals 29 (2010) 220–225.
[16] W. Jiagang, X. Dingquan, W. Yuanyu, W. Lang, J. Yihang, Z. Jianguo, K/Na ratio dependence of the electrical properties of $[(K_xNa_{1-x})0.95-)0.95Li_{0.05}](Nb_{0.95}Ta_{0.05})O_3$ lead-free ceramics, Journal of the American Ceramic Society 91 (2008) 2385–2387.
[17] M. Matsubara, T. Yamaguchi, W. Sakamoto, K. Kikuta, T. Yogo, S.-I. Hirano, Processing and piezoelectric properties of lead-free (K,Na)(Nb,Ta) O_3 ceramics, Journal of the American Ceramic Society 88 (2005) 1190–1196.
[18] M.-R. Yang, C.-S. Hong, C.-C. Tsai, S.-Y. Chu, Effect of sintering temperature on the piezoelectric and ferroelectric characteristics of CuO doped $0.95(Na_{0.5}K_{0.5})NbO_3$–$0.05LiTaO_3$ ceramics, Journal of Alloys and Compounds 488 (2009) 169–173.
[19] Z.-Y. Shen, J.-F. Li, K. Wang, S. Xu, W. Jiang, Q. Deng, Electrical and mechanical properties of fine-grained Li/Ta-modified (Na,K)NbO_3-based piezoceramics prepared by spark plasma sintering, Journal of the American Ceramic Society 93 (2010) 1378–1383.
[20] H.-Y. Park, I.-T. Seo, J.-H. Choi, S. Nahm, H.-G. Lee, Low-temperature sintering and piezoelectric properties of $(Na_{0.5}K_{0.5})NbO_3$ lead-free piezoelectric ceramics, Journal of the American Ceramic Society 93 (2010) 36–39.
[21] G.-Z. Zang, J.-F. Wang, H.-C. Chen, W.-B. Su, C.-M. Wang, P. Qi, B.-Q. Ming, J. Du, L.-M. Zheng, S. Zhang, T.R. Shrout, Perovskite $(Na_{0.5}K_{0.5})_{1-x}(LiSb)_xNb_{1-x}O_3$ lead-free piezoceramics, Applied Physics Letters 88 (2006).
[22] J. Zeng, Y. Zhang, L. Zheng, G. Li, Q. Yin, Enhanced ferroelectric properties of potassium sodium niobate ceramics modified by small amount of $K_3Li_2Nb_5O_{15}$, Journal of the American Ceramic Society 92 (2009) 752–754.
[23] D. Lin, K.W. Kwok, H.L.W. Chan, Structure, dielectric, and piezoelectric properties of CuO-doped $K_{0.5}Na_{0.5}NbO_3$ -BaTi O_3 lead-free ceramics, Journal of Applied Physics 102 (2007).
[24] R.-C. Chang, S.-Y. Chu, Y.-P. Wong, Y.-F. Lin, C.-S. Hong, Properties of $(Na_{0.5}K_{0.5})NbO_3$–$SrTiO_3$ based lead-free ceramics and surface acoustic wave devices, Sensors and Actuators A: Physical 136 (2007) 267–272.
[25] R.-C. Chang, S.-Y. Chu, Y.-F. Lin, C.-S. Hong, Y.-P. Wong, An investigation of $(Na_{0.5}K_{0.5})NbO_3$–$CaTiO_3$ based lead-free ceramics and surface acoustic wave devices, Journal of the European Ceramic Society 27 (2007) 4453–4460.
[26] Y. Wang, L. Qibin, F. Zhao, Phase transition behavior and electrical properties of $[(K_{0.50}Na_{0.50})_{1-x}Ag_x](Nb_{1-x}Ta_x)O_3$ lead-free ceramics, Journal of Alloys and Compounds 489 (2010) 175–178.
[27] R. Zuo, Z. Xu, L. Li, Dielectric and piezoelectric properties of Fe_2O_3-doped $(Na_{0.5}K_{0.5})_{0.96}Li_{0.04}Nb_{0.86}Ta_{0.1}Sb_{0.04}O_3$ lead-free ceramics, Journal of Physics and Chemistry of Solids 69 (2008) 1728–1732.
[28] Q. Zhang, B.-P. Zhang, H.-T. Li, P.-P. Shang, Effects of Sb content on electrical properties of lead-free piezoelectric $[(Na_{0.535}K_{0.480})_{0.942}-Li_{0.058}](Nb_{1-x}Sb_x)O_3$ ceramics, Journal of Alloys and Compounds 490 (2010) 260–263.
[29] D. Lin, K.W. Kwok, H. Tian, H.W.L.-W. Chan, Phase transitions and electrical properties of $(Na_{1-x}K_x)(Nb_{1-y}Sb_y)O_3$ lead-free piezoelectric ceramics with a MnO_2 sintering aid, Journal of the American Ceramic Society 90 (2007) 1458–1462.

[30] M. Dambekalne, M. Antonova, M. Livinsh, A. Kalvane, A. Mishnov, I. Smeltere, R. Krutokhvostov, K. Bormanis, A. Sternberg, Synthesis and characterization of Sb-substituted $(K_{0.5}Na_{0.5})NbO_3$ piezoelectric ceramics, Integrated Ferroelectrics 102 (2008) 52–61.

[31] J. Wu, D. Xiao, Y. Wang, W. Wu, B. Zhang, J. Zhu, $CaTiO_3$-modified $(K_{0.50}Na_{0.50})(Nb_{0.96}Sb_{0.04})O_3$ lead-free piezoelectric ceramics, Journal of the American Ceramic Society 91 (2008) 3402–3404.

[32] H.-Y. Park, I.-T. Seo, M.-K. Choi, S. Nahm, H.-G. Lee, H.-W. Kang, B.-H. Choi, Microstructure and piezoelectric properties of the CuO-added $(Na_{0.5}K_{0.5})$ $(Nb_{0.97}Sb_{0.03})O_3$ lead-free piezoelectric ceramics, Journal of Applied Physics 104 (2008).

[33] L. Su, K. Zhu, L. Bai, J. Qiu, H. Ji, Effects of Sb-doping on the formation of (K, Na)(Nb, Sb)O_3 solid solution under hydrothermal conditions, Journal of Alloys and Compounds 493 (2010) 186–191.

[34] R. Zuo, J. Fu, D. Lv, Y. Liu, Antimony tuned rhombohedral–orthorhombic phase transition and enhanced piezoelectric properties in sodium potassium niobate, Journal of the American Ceramic Society 9999 (2010).

[35] M. Matsubara, T. Yamaguchi, K. Kikuta, S.-I. Hirano, Effect of Li substitution on the piezoelectric properties of potassium sodium niobate ceramics, Japanese Journal of Applied Physics Part 1: Regular Papers Short Notes and Review Papers 44 (2005) 6136–6142.

[36] Z. Yang, X. Chao, C. Kang, R. Zhang, Low temperature sintering and properties of piezoelectric PZT-PFW-PMN ceramics with $YMnO_3$ addition, Materials Research Bulletin 43 (2008) 38–44.

[37] D. Lin, K.W. Kwok, K.H. Lam, H.L.W. Chan, Structure, piezoelectric and ferroelectric properties of Li- and Sb-modified $K_{0.5}Na_{0.5}NbO_3$ lead-free ceramics, Journal of Physics D: Applied Physics 40 (2007) 3500–3505.

[38] K.-I. Kakimoto, K. Akao, Y. Guo, H. Ohsato, Raman scattering study of piezoelectric $(Na_{0.5}K_{0.5})NbO_3$–$LiNbO_3$ ceramics, Japanese Journal of Applied Physics Part 1: Regular Papers Short Notes and Review Papers 44 (2005) 7064–7067.

[39] A.M. Glazer, Simple ways of determining perovskite structures, Acta Crystallographica Section A 31 (1975) 756–762.

[40] M. Ahtee, A.M. Glazer, Lattice parameters and tilted octahedra in sodium–potassium niobate solid solutions, Acta Crystallographica Section A 32 (1976) 434–446.